Axonal plasticity and functional recovery after spinal cord injury in mice deficient in both glial fibrillary acidic protein and vimentin genes

V. Menet*, M. Prieto*, A. Privat*†, and M. Giménez y Ribotta*‡

*Institut National de la Santé et de la Recherche Médicale U 583, Université de Montpellier II, Place E. Bataillon, F-34095 Montpellier Cedex 05, France; and ‡Instituto de Neurociencias, Universidad Miguel Hernandez–Consejo Superior de Investigaciones Científicas, Campus de San Juan, E-03550 San Juan de Alicante, Spain

Communicated by Etienne-Emile Baulieu, Collège de France, Le Kremlin-Bicêtre Cedex, France, May 27, 2003 (received for review January 23, 2003)

The lack of axonal regeneration in the injured adult mammalian spinal cord leads to permanent functional disabilities. The inability of neurons to regenerate their axon is appreciably due to an inhospitable environment made of an astrocytic scar. We generated mice knock-out for glial fibrillary acidic protein and vimentin, the major proteins of the astrocyte cytoskeleton, which are up-regulated in reactive astrocytes. These animals, after a hemisection of the spinal cord, presented reduced astroglial reactivity associated with increased plastic sprouting of supraspinal axons, including the reconstruction of circuits leading to functional restoration. Therefore, improved anatomical and functional recovery in the absence of both proteins highlights the pivotal role of reactive astrocytes in axonal regenerative failure in adult CNS and could lead to new therapies of spinal cord lesions.

The absence of recovery after CNS lesions is a key issue, whose exact mechanisms still await elucidation. Indeed, the lack of spontaneous anatomical and functional repair is due not merely to an intrinsic inability of the neuron to regenerate its injured axon (1) but rather to the presence of a nonneuronal inhospitable local environment in the lesion site constituting a physical and biochemical barrier, the so-called "glial scar" (2). After the lesion, astrocytes undergo hyperplasia, but the main event is an extensive hypertrophy of their cell bodies and cytoplasmic processes. The biochemical hallmark of gliosis is a massive up-regulation of the intermediate filament (IF) protein, glial fibrillary acidic protein (GFAP) (3), which constitutes the structural support of IF in differentiated astrocytes (4), and the reexpression of embryonic IF proteins vimentin (Vim) (5) and nestin (6–8). The functional significance of this postlesional up-regulation of IF proteins is not yet totally established.

To investigate this issue, mice lacking IF proteins, either GFAP (*GFAP*−/−) (9–12) or Vim (*Vim*−/−) (13), were generated by gene targeting. Because there exists a close relationship between GFAP and Vim in reactive astrocytes, it is not excluded that a putative compensation of one protein for the lack of the other could exist. Thus, mice carrying null mutations in both GFAP and Vim genes (double mutant) appeared a particularly interesting tool for studying the potential roles of IF proteins in astrogliosis after injury. Recently, Pekny *et al*. (14) illustrated altered astroglial reaction after transection of dorsal funiculi in double mutant mice compared with those of wild-type (+/+) mice. However, the consequences on axonal plasticity were not investigated. We demonstrated *in vitro* that survival of cortical neurons and neurite growth were improved in coculture with *GFAP*−/− and double mutant spinal cord (SC) (15, 16).

Here, we investigated the *in vivo* counterpart of this interaction in adult mice after complete unilateral hemisection of the SC (17). Because all dorsal and ventral tracts are totally transected on one side of the cord, hemisection yields a permanent unilateral hindlimb functional deficit. In one set of experiments, we analyzed in +/+, *GFAP*−/−, *vim*−/−, and double mutant mice the astroglial reactivity in space and time after the lesion. In another set of experiments, we evaluated the axonal plasticity of two descending systems implicated in locomotor activity and precise motor control. All animals were tested for recovery of motor function in the grid runway test (18), which is particularly appropriate to estimate the hindlimb placement ability of the hemisectioned animals.

We report that, 5 wk postlesion, only the double mutant mice exhibited a significant recovery of locomotor function after complete hemisection of the SC. This significant functional recovery was correlated with reduced glial reactivity in the lesioned side, as compared with wild-type and single mutant mice, and with an extensive plastic sprouting of both serotonergic raphespinal and corticospinal pathways below the lesion level.

Methods

Animals. Three types of mutant mice were used in this study. Mice with null mutations in the GFAP (*GFAP*$^{-/-}$) (10) or Vim genes (*Vim*$^{-/-}$) (13) were crossed to generate double mutant mice. Adult female mice (6–8 mo old) were on a C57BL/6 × DBA/2 × 129sv mixed genetic background. Wild-type counterparts (+/+) were on a C57BL/6 × DBA/2 × 129sv and C57BL/6 × DBA/2 (B6D2) mixed genetic background. A total of 100 animals (n = 25 of each type) were used in this study. Animals were maintained in a conventional animal facility.

SC Injury (SCI). SCI at thoracic level T12 was performed according to our SC hemisection paradigm described in rats (17). Animals were killed after a survival of 3 days, 1, 3, or 5 wk postlesion.

Functional Evaluation. Mice were subjected to the grid runway test to assess locomotor function recovery after the lesion. This test requires accurate limb placement and precise motor control (18, 19). Intact animals classically cross the grid without making footfalls, whereas a hemisectioned animal makes footfalls with the hindlimb ipsilateral to the lesion.

First, mice (n = 7 of each type) were respectively trained for crossing the grid runway twice daily for 5 days before the hemisection. During the second and fourth weeks postlesion, animals were subjected again to the test twice daily for 5 days, and the analysis was performed by averaging the number of footfalls each day.

Labeling of the Corticospinal Tract (CST). For anterograde labeling, 2 days before death at 5 wk postlesion, six mice of each type received three injections (0.15 μl each) of 5% wheat germ agglutinin-conjugated horseradish peroxidase (Sigma) into the ipsilateral sensory-motor cortex (i.e., intact CST). Forty-eight hours later, mice were killed by intracardiac perfusion. Cross

Abbreviations: GFAP, glial fibrillary acidic protein; IF, intermediate filament; Vim, vimentin; SC, spinal cord; SCI, SC injury; CST, corticospinal tract; 5HT, 5-hydroxytryptamine (serotonin); IR, immunoreactive.

†To whom correspondence should be addressed. E-mail: u336@univ-montp2.fr.

sections (30 μm) at the lumbar level were performed and incubated with tetramethylbenzidine as described (20).

For retrograde labeling, 2 days before death, four mice of each type received one injection (0.2 μl) of 2% fast blue (Sigma) at the lumbar level. The mice were killed by intracardiac perfusion, and cross sections (30 μm) were performed through the sensory motor cortex and examined under UV light.

Immunocytochemistry. Three days ($n = 4$), 1 wk ($n = 7$), 3 wk ($n = 7$), or 5 wk ($n = 7$) after hemisection, all animals were deeply anesthetized by an overdose of pentobarbital and intracardially perfused with 0.9% saline followed by either 4% paraformadehyde in 0.1 M phosphate buffer (for nestin immunodetection) or 5% glutaraldehyde in cacodylate (50 mM) sodium metabisulfite buffer [for 5-hydroxytryptamine (serotonin) (5HT) immunodetection]. Cross sections (50 μm) were performed from 2 to 5 mm below the lesion and incubated with primary rabbit antibodies directed against nestin (1/1,000, a gift from R. D. McKay, National Institute of Neurological Disorders and Stroke, Bethesda), S-100 β (1/1,000, Sigma) and 5HT (1/10,000, a gift from M. Geffard, Institut National de la Santé et de la Recherche Médicale, Bordeaux). Antigens were immunodetected by using the peroxidase–antiperoxidase system (16).

Immunoelectron Microscopy. Selected sections below the lesion level at the lumbar level immunostained for 5HT (5 wk after the hemisection) were postfixed with 1% osmium tetroxide in 0.1 M phosphate buffer and embedded in Araldite (Sigma). Ultrathin sections (80 nm) from the ventral horn of both lesioned and intact sides were cut, counterstained with uranyl acetate, and analyzed with a Zeiss 900 electron microscope.

Quantification of Axonal Density and Astrocyte Reactivity. Five weeks after hemisection, the density of immunoreactive (IR) fibers was analyzed and measured on cross sections on both sides of the cord by using the SAMBA 2005 program (Unilog, Meylan, France).

The axonal density was expressed as the surface occupied by serotonergic fibers in the ventral horn on the lesioned side of the cord and CST fibers close to the midline ($n = 6$).

To compensate for 5HT-IR and CST tracing efficiencies in individual animals, mean values of the surface occupied by the fibers on the sectioned side of the cord (six to eight sections per animal) were normalized to that of the contralateral intact side, which constitutes an internal control.

In the same way, the astrocyte reactivity measured by nestin-IR surface on the lesioned side was expressed as a percentage of that on the intact side of the cord ($n = 4$).

Statistics. Statistical significance was evaluated by using the nonparametric Mann–Whitney U test and two-way ANOVA interpretation. The differences were considered significant if P values were <0.05, <0.01, or <0.001. All $\pm$ values indicate SEM.

Results

Locomotor Function Recovery Is Improved in Double Mutant Mice. During the preoperative training period, all mice were able to cross the grid almost with no footfalls (on average, less than one false step per crossing). The animals were then evaluated for locomotor recovery during the second and the fourth weeks after the hemisection.

During the second week after hemisection, both +/+ and double mutant mice were able to cross the grid but without accurate placing of the ipsilateral hindlimb, resulting in footfalls through the holes. They took a significantly longer time to cross the grid: from 12.59 ± 1.1 s to 23.16 ± 5.1 s for +/+ mice and from 11.78 ± 0.99 s to 26.10 ± 1.16 s for double mutant mice (Fig. 1*A*). Moreover, footfalls in the grid runway were not significantly different between +/+ and double mutant mice (Fig. 1*B*).

A	Training period	2 weeks postlesion	4 weeks postlesion
Wild type	12.59 ± 1.1 s	23.16 ± 5.1 s	21.43 ± 2.6 s
Double mutant	11.78 ± 1.0 s	26.10 ± 1.2 s	23.99 ± 3.8 s

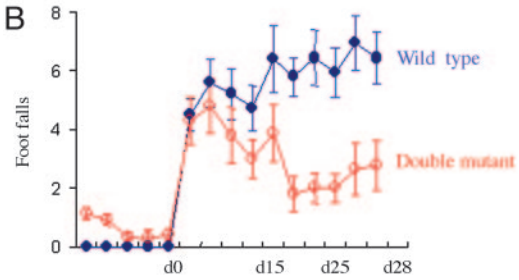

Fig. 1. Behavioral recovery is improved in double mutant mice. (*A*) Time to cross the grid was evaluated during the training period before the SCI and the second and fourth weeks after hemisection. Wild-type and double mutant mice took a significantly longer time to cross the grid after the lesion ($P < 0.001$, Mann–Whitney U test). (*B*) Numbers of footfalls of the impaired hindlimb made by wild-type and double mutant mice were evaluated during the second and fourth weeks after the hemisection ($n = 7$). Error bars indicate standard errors.

During the fourth week after hemisection, the time to cross the grid was unchanged with a mean of 21.43 ± 2.65 s for +/+ mice and 23.99 ± 3.79 s for double mutants (Fig. 1*A*). Moreover, the +/+ mice did not improve and even tended to increase their number of false steps. At variance, the double mutant mice demonstrated a better placement of their impaired hindlimb by significantly decreasing their footfalls ($P < 0.05$, Fig. 1*B*). Indeed, at day 28, the main number of footfalls in +/+ mice was 6.43 ± 0.81 compared with 2.79 ± 0.81 in double mutant mice. The two-way ANOVA test revealed that, between days 14 and 28, there exists a significant decrease of footfalls in double mutant mice, at variance with +/+ mice ($P < 0.0001$). This time course is coherent with the structural plasticity evidenced by our anatomical study.

Anatomical Substrate of the Functional Recovery. Three days to 5 wk after hemisection, astroglial reactivity was investigated by nestin-IR (Fig. 2).

Three days after hemisection, nestin-IR was detected in the vicinity of the lesion in both +/+ and double mutant mice. In +/+ mice, nestin-IR was strictly confined to the lesioned side and intensely decorated bundles of glial filaments in the perikarya and processes of reactive astrocytes in both gray and white matter (Fig. 2*A*). In contrast, in double mutant mice, nestin-IR was overall less marked but appeared in both intact and lesioned sides (Fig. 2*B*). Moreover, nestin-IR was strictly present in the perikarya of astrocytes and decorated neither their processes nor those of the ependymal cells in the central canal (Fig. 2*B*, arrowheads) as in +/+ mice (Fig. 2*A*, arrowheads).

The quantification of the surface occupied by nestin-IR astrocytes confirmed these observations with a lesser increase of nestin-IR in double mutant astrocytes than in those of +/+ mice (2.46 ± 0.34% vs. 8.20 ± 0.55%; $P < 0.001$, Mann–Whitney U test).

One week after hemisection, nestin-IR was less intense in the vicinity of the lesion in both +/+ and double mutant mice. Nestin-positive cells were still detected in the lesioned side of +/+ mice in both the gray and white matter as well as in

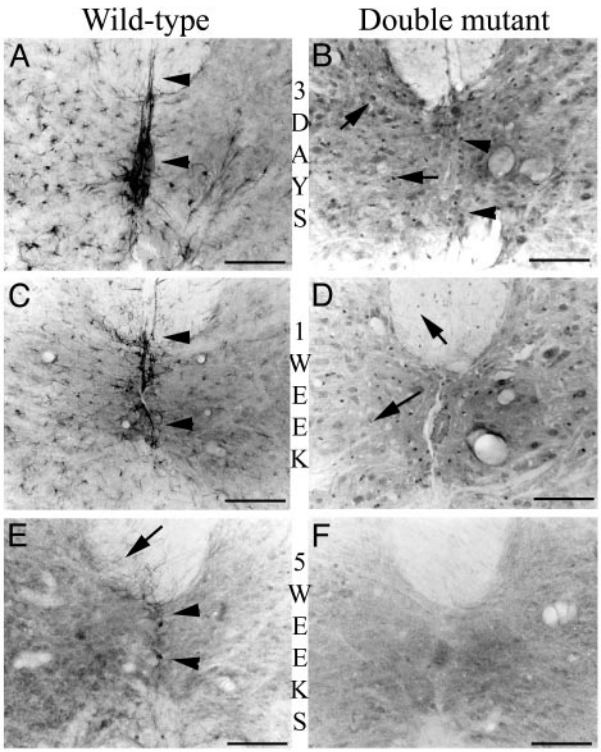

Fig. 2. Astrocyte reactivity is reduced in space and time in double mutant mice. Three days after the lesion (*A* and *B*), nestin-IR is confined to the lesioned side of the cord in a wild-type mouse (*A*), whereas a more diffuse pattern is observed in a double mutant mouse (*B*, arrows). We can observe the differential pattern expression in astrocytes and ependymal cells of a wild-type mouse (*A*, arrowheads) and of double mutant mice (*B*, arrows and arrowheads). One week after the lesion (*C* and *D*), nestin-IR is still present in the lesioned side of the cord of the wild-type mouse decorating the astrocytes processes and the ependymal cells (*C*, arrowheads), whereas it appears more restricted in a double mutant mouse, labeling only few perikarya of astrocytes in the gray and white lesioned matter of the cord (*D*, arrows). Five weeks after the lesion (*E* and *F*), nestin-positive cells are still present in the lesioned side of the cord of the wild-type mouse (*E*), predominantly in the white matter (arrow) and in the ependymal cells (arrowheads). In contrast, no nestin-IR cells are detected in a double mutant mouse (*F*). [Bar (*A* and *B*) = 75 μm.]

ependymal cells (Fig. 2*C*, arrowhead), whereas they were now barely detected in double mutant mice (Fig. 2*D*, arrows). The quantification of the surface occupied by nestin-IR astrocytes confirmed these observations with 7.04 ± 0.33% of the surface detected in the contralateral side in +/+ mice vs. 2.00 ± 0.24% in double mutants ($P < 0.001$, Mann–Whitney *U* test).

Finally, 5 wk after the lesion, nestin-IR persisted in +/+ mice in the white matter of the lesioned side (Fig. 2*E*), particularly in the dorsal (arrow) and ventral funiculi and in ependymal cells, substantiating the presence of a glial scar (Fig. 2*E*, arrowheads). Conversely, in double mutant mice, nestin-IR was undetectable 5 wk after the lesion, indicative of a minimal glial reactivity (Fig. 2*F*).

Reduced astroglial reactivity was confirmed with immunocytochemical detection of an another glial marker, S100 β, which demonstrated a similar modification of pattern of nestin-IR in the different types of mice (data not shown). By comparison, at the same time point, in $Vim^{-/-}$ and in $GFAP^{-/-}$ mice, nestin-IR was comparable with that observed in +/+ mice.

Reinnervation of the Lesioned Cord by Descending Supraspinal Fibers. Two descending supraspinal pathways directly implicated in locomotor activity were analyzed: on one hand, the serotonergic system, which is known to be responsible for modulation and locomotor rhythm production in the SC (21–23) and, on the other hand, the CST, which controls locomotion and contact placing responses (24). To evaluate the reinnervation of the lesioned side, below the lesion, the percentage of the surface occupied by labeled axonal profiles was quantified either in the ventral horns (5HT) or in the vicinity of the midline (CST) on both sides of the SC.

Serotonergic Tract (Fig. 3). In intact SC of +/+ and double mutant animals, 5HT-IR profiles are present in the ventral horn and outline their targets (i.e., the motorneurons; Fig. 3 *A* and *B*).

Three days after hemisection, caudal to the lesion, 5HT-IR was dramatically reduced on the lesioned side of the SC in +/+ mice (Fig. 3*C*) and more so in double mutant mice (Fig. 3*E*), in which only a few coarse varicosities were observed in the ventral horn (arrows). 5HT-IR was also substantially reduced on the intact side in both +/+ (Fig. 3*D*) and double mutant mice (Fig. 3*F*, arrows).

Three weeks after the lesion, 5HT-IR was slightly increased on the lesioned side of the SC in +/+ mice, where some coarse fibers could be observed (Fig. 3*G*, arrows). In contrast, in double mutant mice, numerous thin fibers were present on the lesioned side in the vicinity of the motoneurons (Fig. 3*I*, arrowheads). As expected, 5HT-IR returned progressively to control values on the intact side of both +/+ (Fig. 3*H*) and double mutant mice (Fig. 3*J*).

Five weeks after the lesion, a minimal increase of 5HT-IR was observed on the lesioned side of +/+ mice with some coarse fibers (Fig. 3*K*, arrows), whereas a substantial increase of 5HT-IR was observed on the lesioned side of the double mutant mice all over the ventral horn (Fig. 3*M*). In all animals, the intact side returned to preoperative status at 5 wk (Fig. 3 *L* and *N*).

The quantification of the surface occupied by 5HT-IR fibers (Fig. 4) confirmed these observations with a minimal increase which amounted 46.9 ± 4.7% of the surface detected in the contralateral side in +/+ mice. The picture was similar in $GFAP^{-/-}$ or $vim^{-/-}$ mice with, respectively, 37.3 ± 5.4% and 33.4 ± 3.5% of that detected in the respective contralateral sides. At variance, in double mutant mice, reinnervation reached 77.7 ± 12.8% of the intact side, with a statistically significant increase vs. +/+, *GFAP*−/− and *vim*−/− injured mice ($P < 0.001$, Mann–Whitney *U* test).

Ultrastructural analysis (Fig. 5) illustrated in the intact double mutant mice extensive extracellular spaces not filled by astrocytic processes (Fig. 5*B*, arrowheads). One week (Fig. 5 *C* and *D*) and 5 wk after the lesion (Fig. 5 *E* and *F*), the cellular organization on the lesioned side was altered in both +/+ and double mutant mice with increased extracellular spaces in the ventral horn (arrowheads).

One week after the lesion, 5HT-IR boutons were scarce in +/+ mice (Fig. 5*C*) compared with double mutants. In the latter, they were not ensheathed by astrocytic processes (Fig. 5*D*, arrowheads).

Five weeks after the lesion in double mutant mice, 5HT boutons made synapses on dendrites in the ventral horn (Fig. 5*F*, arrows), and IR profiles were found in direct contact with the basal lamina of blood vessels (Fig. 5*G*), which is completely covered by astrocytic endfeet in +/+ mice.

CST (Fig. 6). Five weeks after hemisection, retrograde labeling of both CSTs with Fast blue injected under the hemisection at lumbar level showed little if any label in the contralateral sensorimotor cortex, thus ruling out a substantial ipsilateral regeneration (data not shown). We labeled the intact CST by anterograde ipsilateral injection of wheat germ agglutinin-conjugated horseradish peroxidase, to detect a possible sprouting from the intact side to the denervated one.

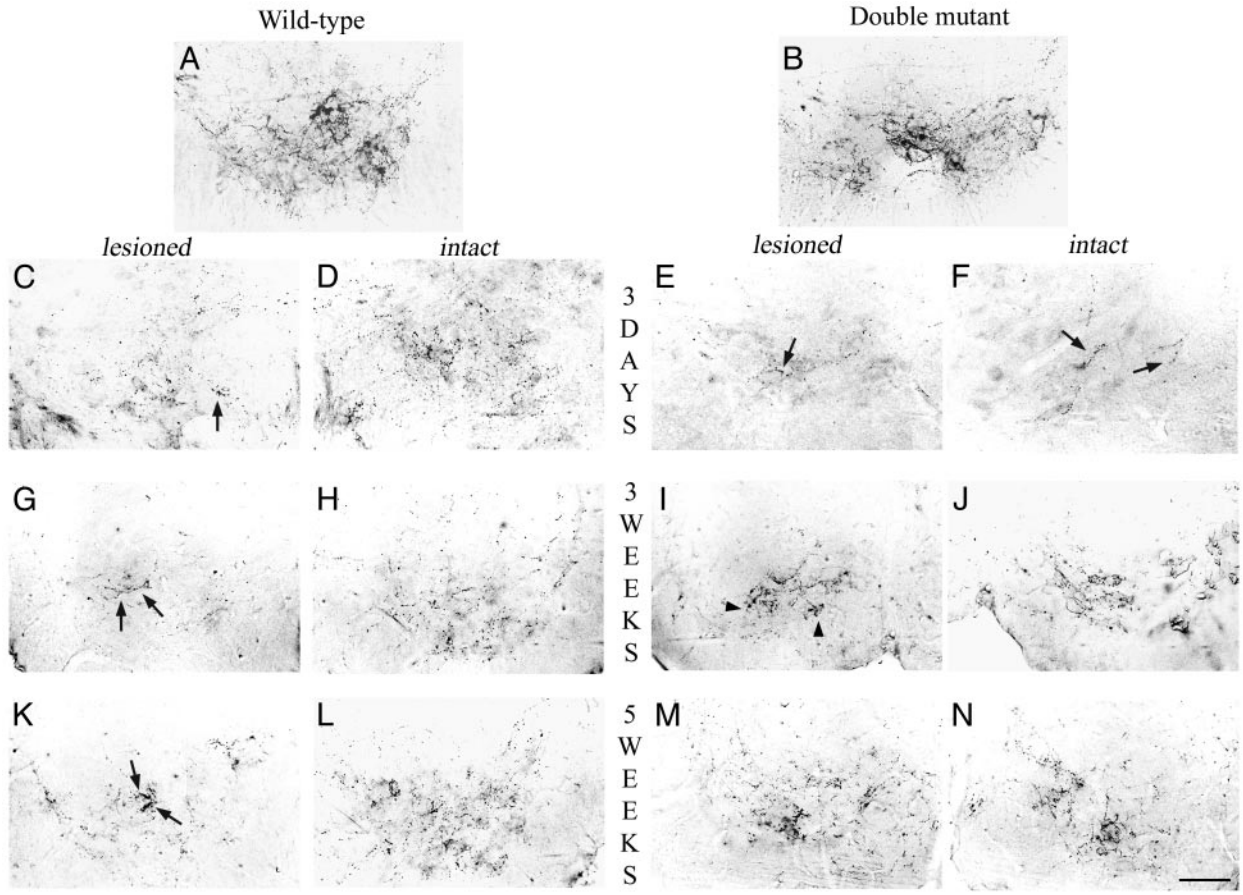

Fig. 3. Immunochemical detection of serotonergic system below the lesion level. In intact wild-type (*A*) and double mutant (*B*) mice, 5HT-IR fibers are present all over the ventral horn of the cord and outline the motoneurons. Three days after hemisection (*C–F*), a substantial decrease of 5HT-IR was observed in the ventral horn on the lesioned side (*C* and *E*) compared with the intact side (*D* and *F*), in both wild-type (*C* and *D*) and double mutant (*E* and *F*) mice. This decreased 5HT-IR was more dramatic in both ventral horns of the double mutant mice (*E* and *F*, arrows). Three weeks after hemisection (*G–J*), a moderate increase of 5HT-IR with coarse fibers was observed in the ventral horn on the lesioned side in wild-type mice (*G*, arrow), whereas a substantial increase of 5HT-IR was observed on the lesioned side of double mutant mice with thin fibers delineating the motoneurons (*I*, arrowheads). 5HT-IR on the intact side of wild-type (*H*) and double mutant (*J*) mice tends to return progressively to control values. Five weeks after the lesion (*K–N*), scarce IR fibers were observed invading the ventral horn on the lesioned side in wild-type mice (*K*, arrows). In contrast, numerous thin 5HT-IR fibers coming from the intact side can be seen on the lesioned side of a double mutant mouse (*M*) where they outline their target, the motoneurons. 5HT-IR on the intact side went back to control value in both wild-type (*L*) and double mutant (*N*) mice and outlines their target, the motoneurons. (Bar = 75 μm.)

Five weeks after hemisection, in the +/+ mice, wheat germ agglutinin-conjugated horseradish peroxidase-labeled CST fibers were detected below the level of the lesion, in the contralateral dorsal funiculus (Fig. 6*A*). They reached the central canal, and few fibers were seen to cross the midline into the denervated areas. This pattern was also observed in both lesioned *vim*$^{-/-}$ (Fig. 6*C*) or *GFAP*$^{-/-}$ (Fig. 6*D*) mice. The fiber density on the lesioned side (Fig. 6*E*) was statistically not different between +/+, *vim*$^{-/-}$, and *GFAP*$^{-/-}$ mice, with a respective mean of 25.53 ± 1.8%, 20.55 ± 2.3%, and 21.43 ± 1.5% of that of the intact side.

In contrast, in double mutant mice (Fig. 6*B*), a significant number of thin fibers was observed to cross the midline from the intact side to the sectioned side of the cord and to extend into the denervated dorsal horn (Fig. 6*B*, arrows). The density of fibers on the lesioned side was significantly increased when compared with +/+, *vim*$^{-/-}$, or *GFAP*$^{-/-}$ mice ($P < 0.001$, Mann–Whitney *U* test) with a mean of 36.33 ± 1.6% of that of the intact side (Fig. 6*E*) due to sprouting from the intact side.

Discussion

The absence of axonal regeneration in the injured CNS, notably after a SCI, has been closely linked to the inhibitory cues of a glial scar, composed essentially of "reactive astrocytes."

In this study, we examined whether the absence of the two major astrocytic IF proteins, namely GFAP and Vim, could directly or indirectly favor axonal elongation by affecting the reactive gliosis.

We found that only those mice deficient for both GFAP and Vim recovered substantial locomotor function after a severe SCI. This functional recovery was associated with a reduced astroglial reactivity and an increased axonal sprouting of supraspinal neurons involved in the control of locomotor activity. Interestingly, the sole absence of one of the proteins did not modify the anatomical and functional responses after the SCI.

Mice deficient in both GFAP and Vim genes exhibit a reduced astroglial reactivity after a massive surgical SCI. This reactivity was analyzed by nestin immunodetection because, in the absence of GFAP and Vim, nestin constitutes the best marker of reactive astrocytes after a CNS injury (6–8). Our results confirm and extend those of another study showing a reduced astroglial reaction after a moderate SCI in double mutant mice (14). We also observed at the ultrastructural level that enlarged extracellular spaces were present in the SC of double mutant mice, even in the absence of a lesion. These observations provide direct evidence that, in the absence of both GFAP and Vim, the

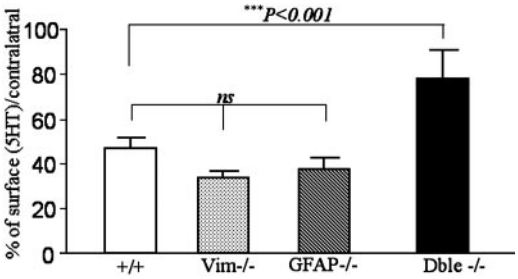

Fig. 4. Quantification of the density of 5HT-IR fibers. Five weeks after the lesion, the density of 5HT-IR fibers on the lesioned side was significantly reduced compared with that from the intact side in wild-type, *vim*−/−, and *GFAP*−/− mutant mice. Interestingly, in double mutant mice, the density of 5HT-IR fibers on the lesioned side was statistically more important compared with that of wild-type, *vim*−/−, and *GFAP* −/− mice (***, $P < 0.001$) and not statistically different from that detected on the intact side (not shown). This measure indicates increased 5HT sprouting in the absence of both GFAP and Vim (Mann–Whitney *U* test). Error bars indicate standard errors.

formation and hypertrophy of astrocytic processes is impaired and extend a recent report that the lack of glial filaments modifies astroglial architecture (25). Moreover, we demonstrate that this impaired astroglial reactivity is associated with increased sprouting of supraspinal systems (serotonergic and corticospinal axons), largely from the intact side.

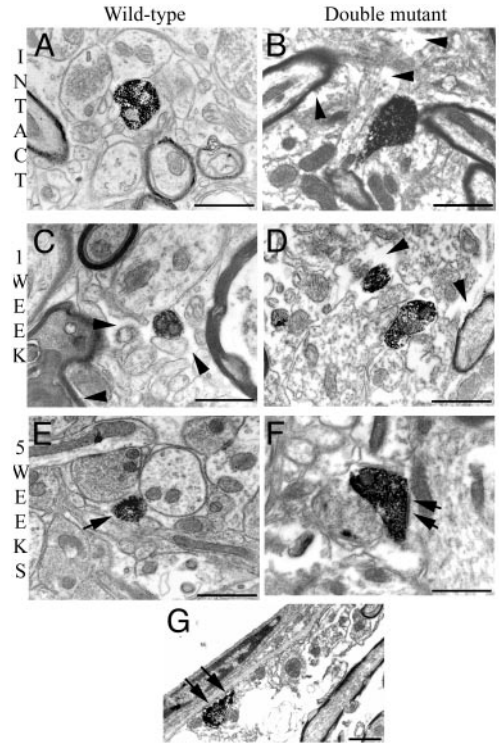

Fig. 5. Ultrastructural organization and serotonergic profiles in the SC below the lesion level. Electron micrographs of a wild-type (*A*, *C*, and *E*) and double mutant (*B*, *D*, and *F*) mouse. An extensive extracellular space can be seen in an intact double mutant mouse (*B*, arrowheads) as compared with that of an intact wild-type animal (*A*). One week after the lesion (*C* and *D*), the ultrastructure on the lesioned side is altered in a wild-type mouse (*C*, arrowheads) but more so in the double mutant one (*D*, arrowheads). Five weeks after the lesion (*E* and *F*), few 5HT-IR profiles can be seen in a wild-type mouse (*E*, arrow), whereas in a double mutant mouse, more abundant 5HT-IR boutons make synaptic contact on dendrites (*F*, arrows) or eventually are directly apposed on the basal lamina of blood vessels (*G*, arrows). (Bars = 1 μm.)

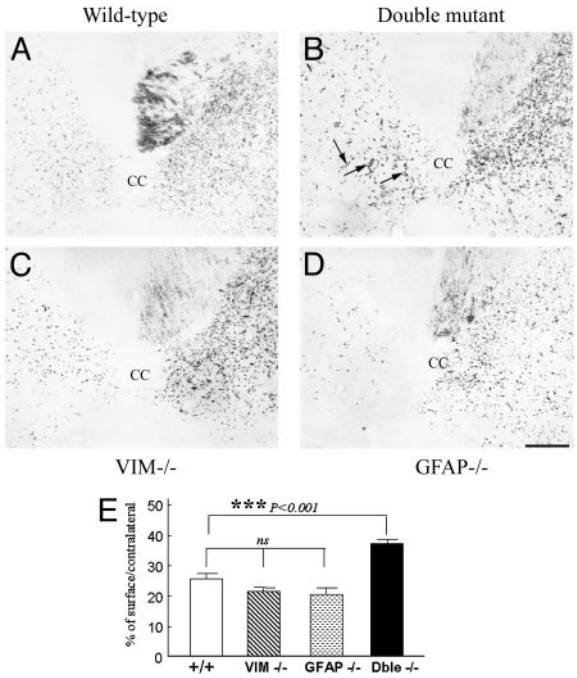

Fig. 6. Anterograde labeling of CST by wheat germ agglutinin-conjugated horseradish peroxidase tracing. (*A–D*) Transverse sections of SC below the lesion level. Few labeled fibers were seen on the lesioned side of the SC in wild-type (*A*), *Vim*−/− (*C*), and *GFAP*−/− (*D*) mice. Observe in a double mutant mouse (arrows, *B*) a significant number of thin fibers that crossed the midline from the intact side to the lesioned side reinnervating the denervated gray matter. (Bar = 50 μm.) (*E*) Quantification of corticospinal sprouting. Fiber density on the lesioned side is expressed as a percentage of that of the intact side and illustrates a significant sprouting of corticospinal fibers only in double mutant mice. ***, $P < 0.001$, Mann–Whitney *U* test. Error bars indicate standard errors.

Thus, the absence of IF proteins modifies the morphological features of reactive astrocytes by abolishing or reducing the physical glial barrier essentially made by their tightly interlinked hypertrophic processes.

These data extend the conclusions of our previous cell culture experiments (15, 16). Indeed, we found that, in the absence of both IF proteins, astrocytes were morphologically immature (16, 25). It is well known that, in the immature CNS, regenerating fibers can grow through lesions (26). This phenomenon seems to be due in part to decreased glial scar formation, thus creating a permissive environment for axonal regeneration (27). Second, we demonstrated *in vitro* that the absence of both IF proteins was associated with biochemical changes in extracellular matrix (ECM) molecules and plasma membranes (16), with improved neuronal survival and increased neuritogenesis. Thus, we can hypothesize that besides modifying the architecture of reactive astrocytes, the absence of GFAP and Vim modifies the balance between permissive ECM molecules and proteoglycans, which are the major molecular constraints within the glial scar (28, 29).

Inherent axonal plasticity does exist in the adult injured supraspinal systems but the postlesional overexpression of both GFAP and Vim, in combination with other factors, is directly or indirectly a key determinant of limited axonal growth after CNS injury. Interestingly, the absence of IFs proteins coincides with an axonal sprouting, which appears 3 and 5 wk after the lesion. Thus, at variance with classical experiments directed at inhibiting myelin-linked obstacle to regeneration (30), we detected little if any ipsilateral long-distance regeneration, but conversely a massive contralateral sprouting of both raphespinal serotonergic and corticospinal axons. This observation is consistent with the

most recent experiments by Bareyre *et al.* (31) and Schwab (32), who also disclosed such sprouting and stated that it could be the substratum of functional improvement.

To analyze the respective contribution of each IF protein, GFAP and Vim, in glial scar formation and consequently on axonal regeneration, experiments were replicated using mice with single null mutation in either the GFAP or Vim gene. Although previous studies have demonstrated phenotypic alterations in mice lacking GFAP (11, 12, 33) or Vim (25, 34), surprisingly we observed no alteration of the astroglial response to a neurological insult in the absence of only one of the two proteins. In parallel, axonal sprouting was not substantially modified. Our results are in accordance with those of Pekny *et al.* (14), which did not observe any difference of astrocyte reaction and those of Wang *et al*. (35), which showed that axonal sprouting was not altered after dorsal hemisection of the SC in the absence of GFAP. These data suggest that GFAP and Vim have partly redundant functions in the astrocytic response contributing to scar formation and consequently in the inhibition of the axonal regeneration.

Finally, the key element to examine after a SCI is recovery of function. We demonstrate here that only double mutant mice significantly recovered motor function of the hindlimb ipsilateral to the lesion when compared with other types of mice. Among numerous methods to assess recovery of locomotor functions, the BBB openfield locomotor rating scale (36) has often been used, because it measures functional changes in voluntary hindlimb movements. However, it must be interpreted very carefully (36), because it is based partly on subjective evaluation and is not homogeneous over the whole scale. The grid runway test appeared to us the most appropriate to evaluate the consequences of a SC hemisection, because it reveals deficits not apparent in general locomotion and requires accurate limb placement, thus reflecting precise substantial motor control (18). The functional recovery observed in double mutant mice apparently results from reorganized lumbosacral circuitry. Indeed, serotonergic and corticospinal axons, which are mainly involved in motor functions, and possibly other axons, sprout from the intact side and establish functional reconnections with denervated targets in the sublesional cord. This finding is in agreement with our recent study demonstrating the existence of a serotonergic drive of the central pattern generator for locomotion (37) in paraplegic rats.

Because we did not evidence any significant regeneration of the ipsilateral CST, our results suggest that the recovery of functions is mainly due to terminal sprouting of spared ipsilateral 5HT terminals or/and that heterotopic sprouting of both 5HT and CST is able to compensate for the initial circuitry. Whatever the case, our experiments shed light on the controversial issue of the origin of functional recovery after partial SC lesions (38, 39) by pointing to sprouting as a key issue in this experimental paradigm, as possibly in many if not all experiments involving partial lesions of the SC.

In summary, we demonstrate here that the modification of the hypertrophic component of astrocyte reactivity to injury and its consequences for adhesive molecules and the extracellular matrix are most appropriate to promote neuronal plasticity after injury and to restore function. This approach is relevant to CNS repair after trauma but also possibly applies to many neurodegenerative diseases, where reactive astrocytes are often part of the neuropathologic substratum. In any case, this model provides an unprecedented tool to study the involvement of astrocytes in the progression of the disease and its functional consequences.

We thank Prof. R. D. McKay for the gift of the Nestin antibody and Drs. C. Babinet, E. Colucci-Guyon, M. Gaviria, and N. Chauvet for valuable discussions. This work was supported by Institut National de la Santé et de la Recherche Médicale, Institut pour la Recherche sur la Moëlle Epinière, and Verticale.

1. David, S. & Aguayo, A. J. (1981) *Science* **214,** 931–933.
2. Reier, P. J., Eng, L. F. & Jakeman, L. (1989) in *Neural Regeneration and Transplantation* (Liss, New York), pp. 183–209.
3. Bignami, A. & Dahl, D. (1976) *Neuropathol. Appl. Neurobiol.* **2,** 99–110.
4. Bignami, A., Eng, L. F., Dahl, D. & Uyeda, C. T. (1972) *Brain Res.* **43,** 429–435.
5. Dahl, D., Rueger, D. C., Bignami, A., Weber, K. & Osborn, M. (1981) *Eur. J. Cell Biol.* **24,** 191–196.
6. Clarke, S. R., Shetty, A. K., Bradley, J. L. & Turner, D. A. (1994) *NeuroReport* **5,** 1885–1888.
7. Lin, R. C., Matesic, D. F., Marvin, M., McKay, R. D. & Brustle, O. (1995) *Neurobiol. Dis.* **2,** 79–85.
8. Frisen, J., Johansson, C. B., Torok, C., Risling, M. & Lendahl, U. (1995) *J. Cell Biol.* **131,** 453–464.
9. Gomi, H., Yokoyama, T., Fujimoto, K., Ikeda, T., Katoh, A., Itoh, T. & Itohara, S. (1995) *Neuron* **14,** 29–41.
10. Pekny, M., Leveen, P., Pekna, M., Eliasson, C., Berthold, C. H., Westermark, B. & Betsholtz, C. (1995) *EMBO J.* **14,** 1590–1598.
11. McCall, A., Gregg, R. G., Behringer, R. R., Brenner, M., Delaney, C. L., Galbreath, E. J., Zhang, C. L., Pearce, R. A., Chiu, S. Y. & Messing, A. (1995) *Proc. Natl. Acad. Sci. USA* **93,** 6361–6366.
12. Liedtke, W., Edelmann, W., Bieri, P. L., Chiu, F. C., Cowan, N. J., Kucherlapati, R. & Raine, C. S. (1996) *Neuron* **17,** 607–615.
13. Colucci-Guyon, E., Portier, M. M., Dunia, I., Paulin, D., Pournin, S. & Babinet, C. (1994) *Cell* **79,** 679–694.
14. Pekny, M., Johansson, C. B., Eliasson, C., Stakeberg, J., Wallen, A., Perlmann, T., Lendahl, U., Betsholtz, C., Berthold, C. H. & Frisen, J. (1999) *J. Cell Biol.* **145,** 503–514.
15. Menet, V., Giménez y Ribotta, M., Sandillon, F. & Privat, A. (2000) *Glia* **31,** 267–272.
16. Menet, V., Giménez y Ribotta, M., Chauvet, N., Drian, M. J., Lannoy, J., Colucci-Guyon, E. & Privat, A. (2001) *J. Neurosci.* **21,** 6147–6158.
17. Giménez y Ribotta, M., Rajaofetra, N., Morin-Richaud, C., Alonso, G., Bochelen, D., Sandillon, F., Legrand, A., Mersel, M. & Privat, A. (1995) *J. Neurosci. Res.* **41,** 79–95.
18. Kunkel-Bagden, E., Dai, H. N. & Bregman, B. (1993) *Exp. Neurol.* **119,** 153–164.
19. Gaviria, M., Haton, H., Sandillon, F. & Privat, A. (2002) *J. Neurotrauma* **19,** 205–221.
20. Arsenio-Nunes, M. L., Sotelo, C. & Wehrle, R. (1988) *J. Comp. Neurol.* **273,** 120–136.
21. Schmidt, B. J. & Jordan, L. M. (2000) *Brain Res. Bull.* **53,** 689–710.
22. Gerin, C. & Privat, A. (1988) *Brain Res.* **794,** 169–173.
23. Jacobs, B. L. & Fornal, C. A. (1997) *Curr. Opin. Neurobiol.* **7,** 820–825.
24. Kunkel-Bagden, E., Dai, H. & Bregman, B. (1992) *Exp. Neurol.* **116,** 40–51.
25. Giménez y Ribotta, M., Langa, F., Menet, V. & Privat, A. (2000) *Glia* **31,** 69–83.
26. Saunders, N. R., Deal, A., Knott, G. W., Varga, Z. M. & Nicholls, J. G. (1995) *Clin. Exp. Pharmacol. Physiol.* **22,** 518–526.
27. Barrett, C. P., Donati, E. J. & Guth, L. (1984) *Exp. Neurol.* **84,** 374–385.
28. Davies, J. A., Goucher, D. R., Doller, C. & Silver, J. (1999) *J. Neurosci.* **19,** 5810–5822.
29. Bradbury, E. J., Moon, L. D., Popat, R. J., King, V. R., Bennett, G. S., Patel, P. N., Fawcett, J. W. & McMahon, S. B. (2002) *Nature* **416,** 636–640.
30. Fouad, K., Dietz, V. & Schwab, M. E. (2001) *Brain Res. Brain Res. Rev.* **36,** 204–212.
31. Bareyre, F. M., Handenschild, B. & Schwab, M. E. (2002) *J. Neurosci.* **22,** 7097–110.
32. Schwab, M. E. (2002) *Prog. Brain Res.* **137,** 351–359.
33. Shibuki, K., Gomi, H., Chen, L., Bao, S., Kim, J. J., Wakatsuki, H., Fujisaki, T., Fujimoto, K., Katoh, A., Ikeda, T., *et al*. (1996) *Neuron* **16,** 587–599.
34. Colucci-Guyon, E., Giménez y Ribotta, M., Maurice, T., Babinet, C. & Privat, A. (1999) *Glia* **25,** 33–43.
35. Wang, X., Messing, A. & David, S. (1997) *Exp. Neurol.* **148,** 568–5776.
36. Privat, A., Giménez y Ribotta, M. & Orsal, D. (2000) *Nat. Med.* **6,** 358.
37. Giménez y Ribotta, M., Provencher, J., Feraboli-Lohnherr, D., Rossignol, S., Privat, A. & Orsal, D. (2000) *J. Neurosci.* **20,** 5144–5152.
38. Bregman, B. S., Kunkel-Bagden, E., Schnell, L., Dai, H. N., Gao, D. & Schwab, M. E. (1995) *Nature* **378,** 498–501.
39. Thallmair, M., Metz, G. A. S., Z'Graggen, W. J., Raineteau, O., Kartje, G. L. & Schwab, M. E. (1998) *Nat. Neurosci.* **1,** 124–131.